Cell cycle heterogeneity directs the timing of neural stem cell activation from quiescence

Authors: L. Otsuki[1], A.H. Brand[1]*

Affiliations:
[1] The Gurdon Institute and Department of Physiology, Development and Neuroscience, University of Cambridge, Tennis Court Road, Cambridge, CB2 1QN, UK.

*Correspondence to: a.brand@gurdon.cam.ac.uk.

Abstract:

Quiescent stem cells in adult tissues can be activated for homeostasis or repair. Neural stem cells (NSCs) in *Drosophila* are reactivated from quiescence in response to nutrition by the insulin signalling pathway. It is widely accepted that quiescent stem cells are arrested in G0. In this study, however, we demonstrate that quiescent NSCs (qNSCs) are arrested in either G2 or G0. G2/G0 heterogeneity directs NSC behavior: G2 qNSCs reactivate before G0 qNSCs. In addition, we show that the evolutionarily conserved pseudokinase Tribbles (Trbl) induces G2 NSCs to enter quiescence by promoting degradation of $Cdc25^{String}$ and subsequently maintains quiescence by inhibiting Akt activation. Insulin signalling overrides repression of Akt and silences *trbl* transcription, allowing NSCs to exit quiescence. Our results have implications for identifying and manipulating quiescent stem cells for regenerative purposes.

One Sentence Summary:

G2-arrested quiescent stem cells reactivate more readily than G0 cells and are regulated by the pseudokinase Tribbles.

As in mammals, NSCs in *Drosophila* proliferate during embryogenesis, become quiescent in the late embryo and then proliferate again (reactivate) post-embryonically to produce neurons and glia (**Fig. 1A**) (*1*, *2*). A nutritional stimulus induces reactivation (*3*); specifically, dietary amino acids induce glial cells in the blood brain barrier to secrete insulin/IGF-like peptides (dILPs) (*4*, *5*). dILPs activate the insulin signalling pathway in neighboring qNSCs, prompting them to exit quiescence (*4*, *6*).

Quiescent stem cells are widely accepted to be arrested in G0, a poorly-understood state characterised by a 2*n* DNA content and a lack of expression of cell cycle progression factors (*7*). We assessed whether *Drosophila* qNSCs are G0-arrested (**Fig. S1A**). As expected, we did not detect the M phase marker phospho-Histone H3 (pH3) in qNSCs (**Fig. S1B**). Previous studies demonstrated that qNSCs do not express the G1 marker Cyclin E, or incorporate the S phase markers BrdU/EdU (*1*, *3*, *6*, *8*). However, we found that 73% of quiescent NSCs express the G2 markers Cyclin A (CycA) and Cyclin B (CycB) (**Figs. 1B, S1C**). This suggests that (i) most qNSCs arrest in G2 and that (ii) qNSCs arrest heterogeneously in the cell cycle.

We verified that ~75% of qNSCs are G2-arrested by comparing the FUCCI/pH3 profiles of qNSCs and proliferating NSCs (**Figs. 1C-D, S1D**) (*9*, *10*). $CycA^+$ qNSCs had twice the DNA content (**Fig. 1E**) and larger nuclei (30.5±0.66μm^3 *vs* 18.1±0.32μm^3, *n*=10 tVNCs, ~75 NSCs each) when compared to $CycA^-$ qNSCs. Thus qNSCs exhibit two types of stem cell quiescence: the majority arrests in G2 and a minority in G0 (**Fig. 1F**). G2 quiescence has not been reported previously in stem cells in mammals or *Drosophila*.

The choice of G2 or G0 arrest could be stochastic or pre-programmed. We found 7 G0 qNSCs in the T1 hemi-segment and 8 G0 qNSCs each in T2 and T3. A consistent subset of qNSCs always arrested in G0, namely NB2-2, NB2-4, NB2-5, NB3-4, NB5-3 and NB7-4 (**Figs. 2A-B, S2A-F, Table S1**). Of these, NB2-4 disappears from T1 during embryogenesis (*11*, *12*), explaining why fewer qNSCs are G0-arrested in T1 than T2/T3. NB5-4/NB5-7 were G2-arrested in 50% of hemi-segments but did not always arrest in the same cell cycle phase either side of the midline (**Fig. S2F**). We conclude that, with the exception of NB5-4 and NB5-7, the choice of G2 or G0 quiescence is entirely invariant.

Is G2/G0 heterogeneity in qNSCs significant? We assessed reactivation of G2 and G0 qNSCs by tracking expression of the reactivation marker *worniu* (*wor*) (**Figs. S3A-C**). Over 86% of G2 qNSCs reactivated by 20 hours after larval hatching (ALH), as compared to 20% of G0 qNSCs (**Fig. 2C**, *n*=10 tVNCs, ~150 NSCs each). For example NB3-4, a G0 qNSC, reactivated in fewer than 7% of hemi-segments (*n*=10 tVNCs, 6 hemi-segments each) (**Fig. 2D**). All NSCs reactivated by 48 hours ALH (**Fig. S3C**). Thus G2 qNSCs are faster-reactivating stem cells than G0 qNSCs.

We next profiled gene expression in qNSCs using Targeted DamID (TaDa) (*13*), identifying 1656 genes with GO terms including 'nervous system development' (35 genes, corrected *p* value: 2.70×10^{-6}) and 'neuroblast (NSC) development' (10 genes, corrected *p* value: 8.40×10^{-4}) (**Tables S2 and S3**). To identify quiescence-specific genes, we eliminated genes common to quiescent and proliferating NSCs (*13*) such as *deadpan* (*dpn*) (**Figs. S4A-B**). *tribbles (trbl)* is one

of the most significantly expressed protein-coding genes specific to qNSCs (**Fig. S4C**). *trbl* encodes an evolutionarily conserved pseudokinase with three human homologues that have been implicated in insulin and MAPK signalling (reviewed by (*14*)). We confirmed that *trbl* labels quiescent but not proliferating NSCs *in vivo* (**Figs. 3A, S4D-F**). To date, no other gene has been identified that labels qNSCs specifically.

trbl is necessary for quiescence entry, as NSCs continued to divide during late embryogenesis in *trbl* hypomorphic mutants or when *trbl* was knocked down specifically in NSCs (**Figs. 3B, S5A-D**). *trbl* regulates quiescence entry specifically, without affecting division mode or cell viability (**Fig. S5E-F).** The ectopically dividing NSCs in the $trbl^{EP3519}$ mutant were G2, not G0, qNSCs (**Fig. S5G**). G2, but not G0, qNSCs also became significantly smaller in $trbl^{EP3519}$ mutants (**Figs. S5H-J**). As embryonic NSCs do not re-grow between cell divisions (*15*), the size reduction is consistent with excessive divisions. Consistent with a function in G2 quiescence, Trbl was expressed primarily in G2 qNSCs (**Figs. 3C, S5K**).

Trbl is also required to maintain quiescence. RNAi-mediated knockdown of *trbl* in qNSCs caused NSCs to leave quiescence and divide (**Fig. S5L-M**). We generated transgenic flies carrying UAS-GFP-Trbl and drove expression with *grainyhead (grh)*-GAL4 (*4*) to assess whether Trbl is sufficient to maintain G2 quiescence. *grh*-GAL4 expression initiates at quiescence entry and is expressed in ~67% of NSCs, allowing comparison between neighboring GFP-Trbl-expressing and non-expressing NSCs. Almost all GFP-Trbl-expressing NSCs remained in G2 quiescence and expressed CycA (91.8±0.88%, n=10 tVNCs, ~120 NSCs each) (**Figs. 3D-E, S6A-C**). GFP-Trbl-expressing NSCs retained the primary process that is extended

specifically by quiescent NSCs (see **Fig. 1A**), unlike control NSCs, which had begun to divide (**Figs. S6B-C**) (*1*, *4*, *16*). Thus Trbl is sufficient to maintain G2 quiescence.

In the embryonic mesoderm, *trbl* induces G2 arrest by promoting $Cdc25^{String}$ protein degradation (*17-19*). We found that $Cdc25^{String}$ protein is reduced in NSCs at quiescence entry whereas $cdc25^{string}$ mRNA is maintained (**Fig. 4A**). Therefore, $Cdc25^{String}$ is regulated post-transcriptionally at quiescence entry. Significantly more NSCs were $Cdc25^{String}$ protein-positive in $trbl^{EP3519}$ mutants (**Figs. 4B, S7A-B**). This increase in $Cdc25^{String}$ is sufficient to explain the excessive NSC proliferation in *trbl* mutants (**Figs. S7C-D**). Thus Trbl initiates quiescence entry by promoting $Cdc25^{String}$ protein degradation during late embryogenesis.

Trbl also maintains NSC quiescence post-embryonically, however, it must act through another mechanism as $Cdc25^{String}$ is no longer expressed in post-embryonic qNSCs (**Fig. S8A**). Trbl is known to inhibit insulin signalling through binding Akt and preventing its phosphorylation (**Fig. S8B**) (*20*). Consistent with this, Trbl-expressing NSCs had less *p*4E-BP than control NSCs (**Fig. S8C**). If Trbl inhibits Akt to maintain quiescence, constitutively active Akt (myr-Akt (*21*); Akt^{ACT}) should rescue Trbl-induced quiescence: Akt^{ACT} fully rescued NSC reactivation (**Figs. 4C, S8D**). In contrast, as Trbl is thought to act downstream of PI3K (*20*), constitutively active PI3K ($dp110^{CAAX}$, (*22*); $PI3K^{ACT}$) should not rescue reactivation, which it did not (**Figs. 4D, S8D**). Thus Trbl maintains quiescence by blocking activation of Akt. This role is specific to post-embryonic NSCs since embryonic NSCs do not depend on insulin signalling to proliferate (**Fig. S8E**).

trbl expression must be repressed to allow NSC reactivation. We found that insulin signalling is necessary and sufficient to repress *trbl* transcription. NSCs misexpressing PTEN, an insulin pathway inhibitor, failed to down-regulate *trbl* transcription (**Fig. S8F**). In contrast, activating the insulin pathway by expressing Akt^{ACT} in NSCs was sufficient to switch off *trbl* transcription (**Fig. S8G**).

Here we have discovered the mechanisms by which *Drosophila* NSCs enter, remain in, and exit quiescence in response to nutrition (**Fig. 4E**). Trbl pseudokinase (1) promotes degradation of $Cdc25^{String}$ protein to induce quiescence, (2) blocks insulin signalling by inhibiting Akt in the same NSCs to maintain quiescence, and (3) is overridden by nutrition-dependent secretion of dILPs from blood-brain barrier glia, which activate insulin signalling in qNSCs, repress *trbl* expression and enable reactivation.

Contrary to the prevailing dogma, we found that qNSCs are pre-programmed to arrest in G2 or G0. G2 qNSCs reactivate earlier and generate neurons before G0 qNSCs; this may ensure that neurons form the correct circuits in the appropriate order during brain development. G2 arrest also enables high fidelity homologous recombination-mediated repair in response to DNA damage, preserving genomic integrity during quiescence. Quiescent stem cells in mammals may also arrest in G2, with implications for isolating and manipulating quiescent stem cells for therapeutic purposes.

References and Notes:

1. J. W. Truman, M. Bate, *Developmental Biology*. **125**, 145–157 (1988).
2. A. Prokop, G. M. Technau, *Development* (1991).
3. J. S. Britton, B. A. Edgar, *Development*. **125**, 2149–2158 (1998).
4. J. M. Chell, A. H. Brand, *Cell*. **143**, 1161–1173 (2010).
5. P. Spéder, A. H. Brand, *Developmental Cell*. **30**, 309–321 (2014).
6. R. Sousa-Nunes, L. L. Yee, A. P. Gould, *Nature*. **471**, 508–512 (2011).
7. T. H. Cheung, T. A. Rando, *Nat. Rev. Mol. Cell Biol.* **14**, 329–340 (2013).
8. S.-L. Lai, C. Q. Doe, *eLife*. **3** (2014), doi:10.7554/eLife.03363.
9. A. Sakaue-Sawano *et al.*, *Cell*. **132**, 487–498 (2008).
10. N. Zielke *et al.*, *Cell Rep*. **7**, 588–598 (2014).
11. J. W. Truman, H. Schuppe, D. Shepherd, D. W. Williams, *Development*. **131**, 5167–5184 (2004).
12. H. Lacin, J. W. Truman, K. VijayRaghavan, *eLife*. **5**, e13399 (2016).
13. T. D. Southall *et al.*, *Developmental Cell*. **26**, 101–112 (2013).
14. P. A. Eyers, K. Keeshan, N. Kannan, *Trends Cell Biol.* (2016), doi:10.1016/j.tcb.2016.11.002.
15. V. Hartenstein, E. Rudloff, J. A. C. Ortega, *Roux's Arch Dev Biol*. **196**, 473–485 (1987).
16. K. Narbonne-Reveau *et al.*, *eLife*. **5**, e13463 (2016).
17. J. Mata, S. Curado, A. Ephrussi, P. Rørth, *Cell*. **101**, 511–522 (2000).
18. J. Grosshans, E. Wieschaus, *Cell*. **101**, 523–531 (2000).
19. T. C. Seher, M. Leptin, *Curr. Biol.* **10**, 623–629 (2000).
20. R. Das, Z. Sebo, L. Pence, L. L. Dobens, *PLoS ONE*. **9**, e109530 (2014).
21. J. S. Britton, W. K. Lockwood, L. Li, S. M. Cohen, B. A. Edgar, *Developmental Cell*. **2**, 239–249 (2002).
22. S. J. Leevers, D. Weinkove, L. K. MacDougall, E. Hafen, M. D. Waterfield, *EMBO J.* **15**, 6584–6594 (1996).

23. J. A. Campos-Ortega, V. Hartenstein, *The Embryonic Origin of Drosophila melanogaster* (1985).

24. A. T. Quiñones-Coello *et al.*, *Genetics*. **175**, 1089–1104 (2007).

25. P. Rørth *et al.*, *Development*. **125**, 1049–1057 (1998).

26. S. Nagarkar-Jaiswal *et al.*, *eLife*. **4**, e05338 (2015).

27. R. Albertson, C. Chabu, A. Sheehan, C. Q. Doe, *J. Cell. Sci.* **117**, 6061–6070 (2004).

28. L. Luo, Y. J. Liao, L. Y. Jan, Y. N. Jan, *Genes & Development*. **8**, 1787–1802 (1994).

29. T. Lee, L. Luo, *Neuron*. **22**, 451–461 (1999).

30. S. E. McGuire, P. T. Le, A. J. Osborn, K. Matsumoto, R. L. Davis, *Science*. **302**, 1765–1768 (2003).

31. H. Huang *et al.*, *Development*. **126**, 5365–5372 (1999).

32. A. Estacio-Gómez *et al.*, *Development*. **140**, 2139–2148 (2013).

33. H.-H. Li *et al.*, *Cell Rep*. **8**, 897–908 (2014).

34. S. Di Talia *et al.*, *Curr. Biol.* **23**, 127–132 (2013).

35. W. G. Whitfield, C. Gonzalez, G. Maldonado-Codina, D. M. Glover, *EMBO J.* **9**, 2563–2572 (1990).

36. R. Dittrich, T. Bossing, A. P. Gould, G. M. Technau, J. Urban, *Development*. **124**, 2515–2525 (1997).

37. D. Kosman, S. Small, J. Reinitz, *Dev. Genes Evol.* **208**, 290–294 (1998).

38. T. Isshiki, M. Takeichi, A. Nose, *Development*. **124**, 3099–3109 (1997).

39. S. Rozen, H. Skaletsky, *Methods Mol. Biol.* **132**, 365–386 (2000).

40. K. H. Cox, D. V. DeLeon, L. M. Angerer, R. C. Angerer, *Developmental Biology*. **101**, 485–502 (1984).

41. G. S. Wilkie, A. W. Shermoen, P. H. O'Farrell, I. Davis, *Curr. Biol.* **9**, 1263–1266 (1999).

Acknowledgments:

We thank P. Callaerts, F. Díaz-Benjumea, J. Dods, C. Q. Doe, B. Edgar, E. Higginbotham, Y. Kimata, J. Ng, J. Urban, U. Walldorf, E. Wieschaus, Bloomington *Drosophila* Stock Centre and Developmental Studies Hybridoma Bank (DSHB) for generously providing reagents; T. Southall and O. J. Marshall for updating the TaDa microarray data to Release 6 of the *Drosophila* genome and for gene expression analysis; F. Doetsch, A. C. Delgado, F. J. Livesey, D. St. Johnston and the Brand laboratory members for discussion. Funding: This work was funded by the Royal Society Darwin Trust Research Professorship, Wellcome Trust Senior Investigator Award 103792 and Wellcome Trust Programme grant 092545 to A.H.B., and Wellcome Trust PhD Studentship 097423 to L.O. A.H.B acknowledges core funding to the Gurdon Institute from the Wellcome Trust (092096) and CRUK (C6946/A14492). Author contributions: L.O. and A.H.B. designed the experiments, analysed the data and wrote the manuscript. L.O. performed the experiments. Competing interests: The authors declare no conflict of interest. Data and Materials accessibility: Microarray data have been deposited with GEO: accession GSE81745.

Supplementary Materials:

Materials and Methods

Figures S1-S8

Tables S1

References (*23-41*)

Additional data tables S2-S3 (separate files)

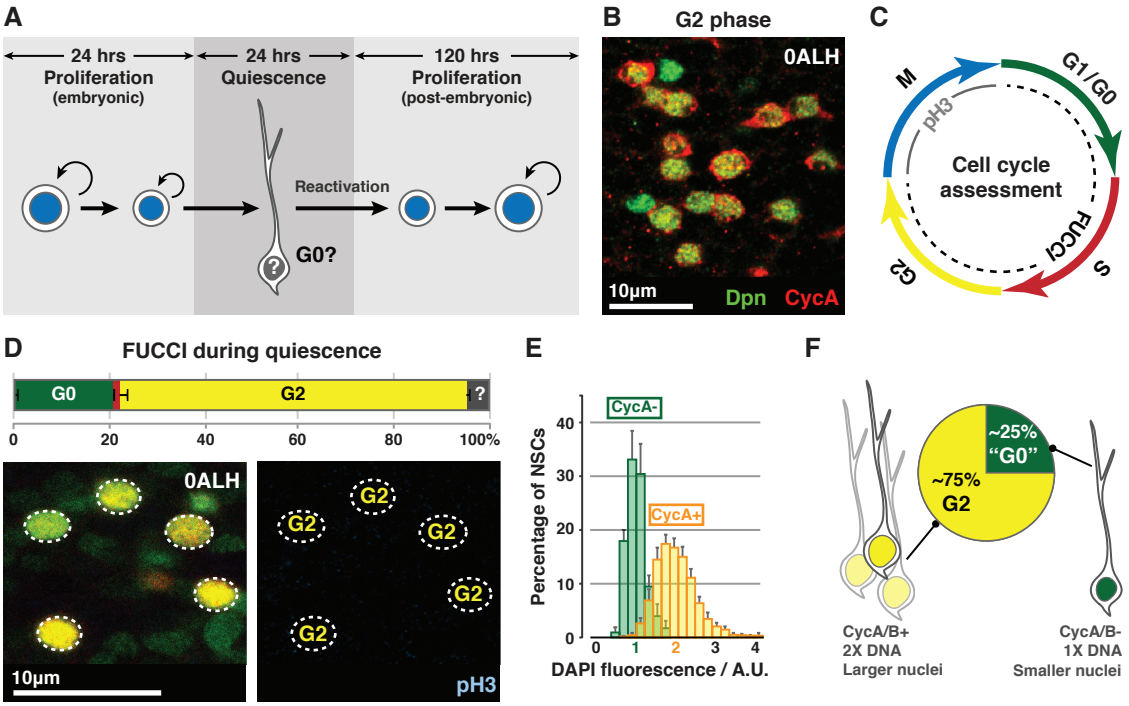
A
24 hrs
Proliferation
(embryonic)
24 hrs
Quiescence
120 hrs
Proliferation
(post-embryonic)
Reactivation
G0?
B
G2 phase
0ALH
10µm
Dpn
CycA
C
M
G1/G0
S
G2
pH3
FUCCI
Cell cycle
assessment
D
FUCCI during quiescence
G0
G2
?
0
20
40
60
80
100%
0ALH
10µm
G2
pH3
E
CycA-
CycA+
Percentage of NSCs
DAPI fluorescence / A.U.
F
~25%
"G0"
~75%
G2
CycA/B+
2X DNA
Larger nuclei
CycA/B-
1X DNA
Smaller nuclei

Figure 1

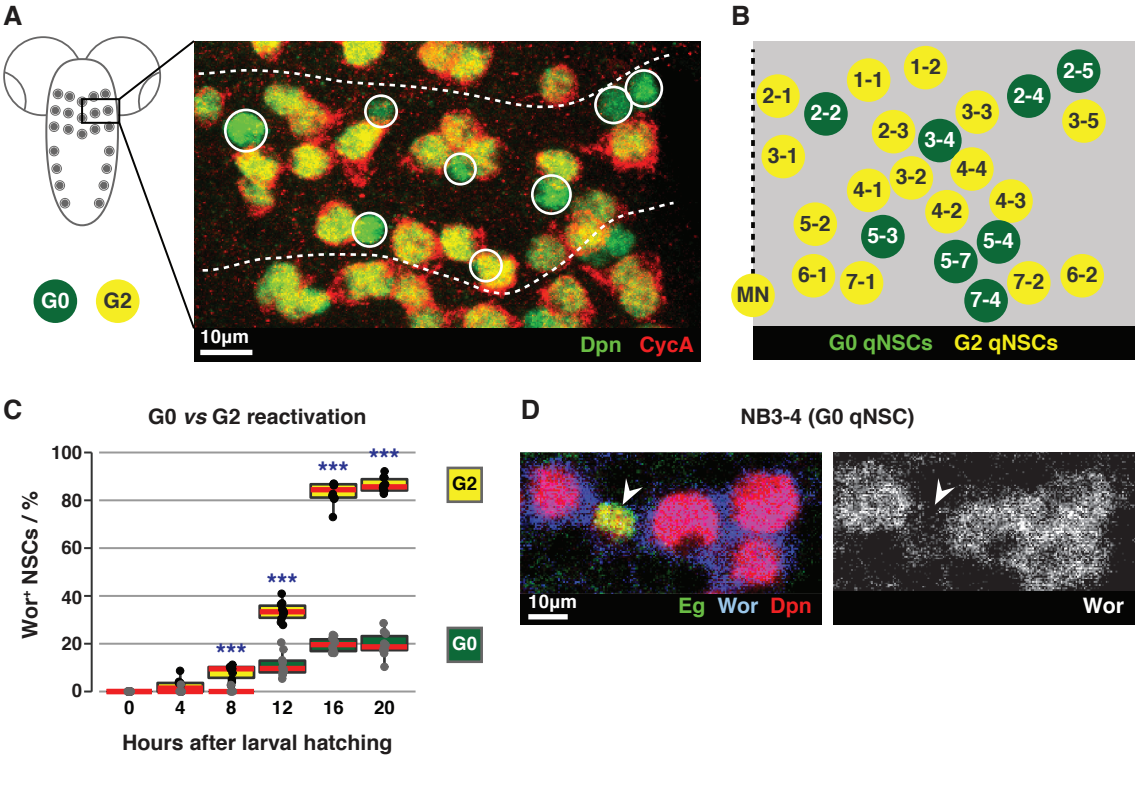
A
G0
G2
10µm
Dpn CycA
B
1-1
1-2
2-1
2-2
2-3
2-4
2-5
3-1
3-2
3-3
3-4
3-5
4-1
4-2
4-3
4-4
5-2
5-3
5-4
5-7
6-1
6-2
7-1
7-2
7-4
MN
G0 qNSCs G2 qNSCs
C
G0 vs G2 reactivation
Wor+ NSCs / %
100
80
60
40
20
0
0 4 8 12 16 20
Hours after larval hatching
***
G2
G0
D
NB3-4 (G0 qNSC)
10µm
Eg Wor Dpn
Wor

Figure 2

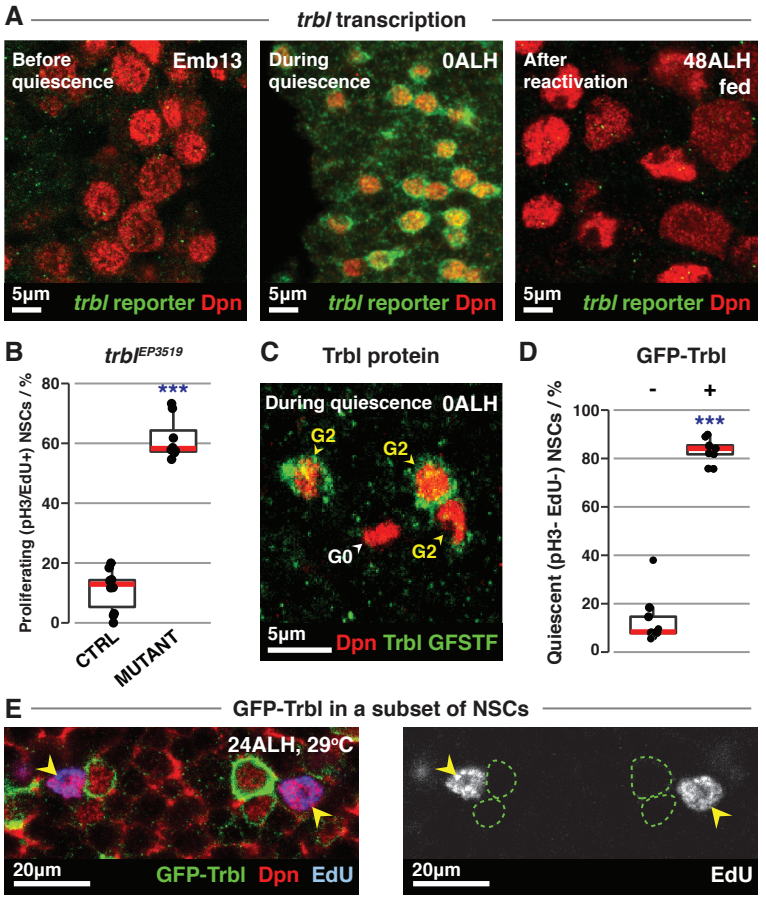
A
trbl transcription
Before quiescence
Emb13
During quiescence
0ALH
After reactivation
48ALH fed
5μm
trbl reporter Dpn
B
trbl EP3519
Proliferating (pH3/EdU+) NSCs / %
***
CTRL
MUTANT
C
Trbl protein
During quiescence 0ALH
G2
G0
5μm
Dpn Trbl GFSTF
D
GFP-Trbl
Quiescent (pH3- EdU-) NSCs / %
E
GFP-Trbl in a subset of NSCs
24ALH, 29°C
20μm
GFP-Trbl Dpn EdU
EdU

Figure 3

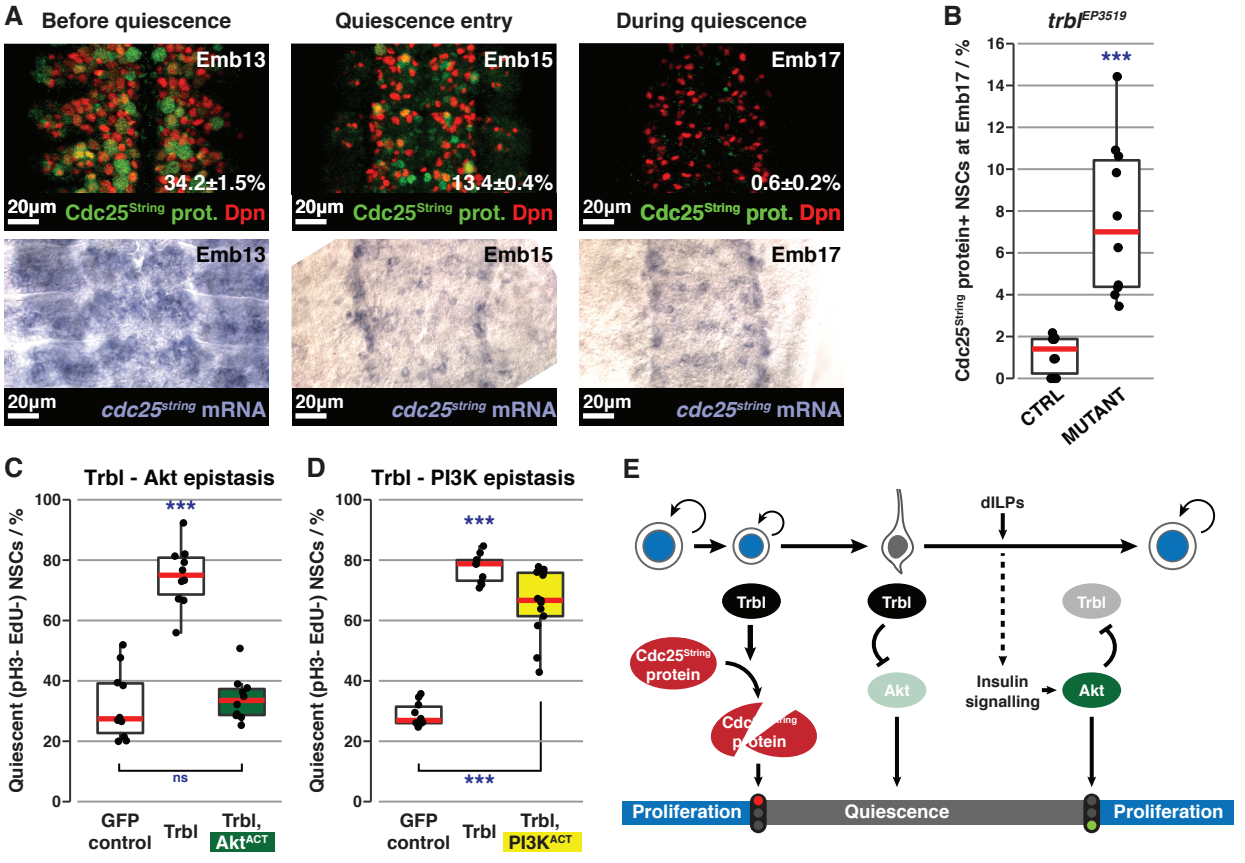
A
Before quiescence
Quiescence entry
During quiescence
Emb13
Emb15
Emb17
34.2±1.5%
13.4±0.4%
0.6±0.2%
20µm
Cdc25String prot. Dpn
cdc25string mRNA
B
trblEP3519
***
Cdc25String protein+ NSCs at Emb17 / %
CTRL
MUTANT
C
Trbl - Akt epistasis
Quiescent (pH3- EdU-) NSCs / %
ns
GFP control
Trbl
Trbl, AktACT
D
Trbl - PI3K epistasis
Trbl, PI3KACT
E
dILPs
Trbl
Cdc25String protein
Akt
Insulin signalling
Proliferation
Quiescence

Figure 4

Figure Legends:

Fig. 1. qNSCs arrest in G0 or G2.

(**A**) qNSCs are smaller than proliferating NSCs and extend a primary process, which is retracted upon activation from quiescence. Proliferating NSCs in the embryo do not exhibit a primary process prior to entering quiescence.

(**B**) 73±0.79% of qNSCs (green) are $CycA^+$ (red). *n*=10 tVNCs, ~150 NSCs each.

(**C**) Cell cycle phase assessment using FUCCI and pH3.

(**D**) Percentages of NSCs (outlined) in each cell cycle phase during quiescence. Colours as in (C). *n*=5 tVNCs, ~150 NSCs each. ?: undetermined.

(**E**) DAPI intensities of $CycA^+$ and $CycA^-$ qNSC nuclei are significantly different ($p=2.20x10^{-16}$, Kolgomorov-Smirnov test). *n*=10 tVNCs, ~75 NSCs each. A.U.: arbitrary units. 1 A.U.: mean DAPI intensity of the $CycA^-$ population. Error bars indicate S.E.M.

(**F**) Features of G2 and G0 qNSCs.

Images are single section confocal images, unless indicated otherwise, and anterior is up in this and all subsequent figures.

Fig. 2. G2 qNSCs reactivate before G0 qNSCs.

(**A**) Maximum intensity projection of a tVNC hemi-segment, stained for G2 (yellow) and G0 (green; circled) qNSCs. Dotted lines indicate hemi-segment boundaries.

(**B**) Positions and identities of G0 qNSCs (green) within a hemi-segment. Dotted line represents the midline. Schematic modified from (*12*).

(**C**) Quantification of Wor^+ G0 or G2 qNSCs. n=10 tVNCs/time point, ~150 NSCs each. ***: $p<1.39x10^{-5}$, two-tailed paired t-tests. Red lines indicate medians.

(**D**) NB3-4 (Eg^+; arrowed), remains small and Wor-negative at 20ALH, while neighbouring G2 qNSCs have reactivated.

Fig. 3. *trbl* regulates G2 qNSCs.

(**A**) *trbl* reporter expression (green) in NSCs (red) before, during and after quiescence.

(**B**) Quantification of proliferating NSCs in control (n=10) *vs* $trbl^{EP3519}$ mutant (n=8) tVNCs, with ~120 NSCs each. ***: $p=7.06\text{x}10^{-14}$, Student's t-test.

(**C**) Trbl protein expression (green) in G2 ($CycA^{+}$) or G0 ($CycA^{-}$) qNSCs (red).

(**D**) Quantification of qNSCs in *grh*-GAL4>GFP-Trbl tVNCs. "-" and "+" denote $GFP\text{-}Trbl^{-}$ and $GFP\text{-}Trbl^{+}$ NSCs respectively. n=9 tVNCs, ~150 NSCs each. ***: $p=3.90\text{x}10^{-4}$, Wilcoxon signed-rank test.

(**E**) In *grh*-GAL4>GFP-Trbl brains, $GFP\text{-}Trbl^{+}$ NSCs (green outlines) do not incorporate EdU, while control NSCs (yellow arrowheads) do.

Red lines indicate medians.

Fig. 4. Trbl induces and maintains quiescence through different mechanisms.

(**A**) Top row: $Cdc25^{String}$ protein (green) expression in NSCs (red) before and during quiescence (percentages are mean±SEM). *n*=10 tVNCs/time point, ~130 NSCs each. Maximum intensity projections. Bottom row: *In situ* hybridisation against $cdc25^{string}$ mRNA at the same stages.

(**B**) Percentages of $Cdc25^{String}$ $protein^{+}$ NSCs in control ($trbl^{EP3519}$ heterozygote) *vs* mutant tVNCs. *n*=10 tVNCs/genotype, ~110 NSCs each. ***: $p=9.08x10^{-5}$, Kolgomorov-Smirnov test.

(**C** and **D**) Quantification of qNSCs in epistasis experiments between GFP-Trbl and Akt^{ACT} (C) or $PI3K^{ACT}$ (D). *n*>10 tVNCs/condition, ~80 NSCs each. ***: $p<3.39x10^{-9}$. *ns*: $p>0.05$, one way ANOVA followed by post-hoc Tukey's HSD test. In (D), there is no significant difference between GFP-Trbl alone and GFP-Trbl+$PI3K^{ACT}$.

(**E**) Three-step model for Trbl activity.

Red lines indicate medians.

Supplementary Materials for

Cell cycle heterogeneity directs the timing of neural stem cell activation from quiescence

Authors: L. Otsuki, A.H. Brand

correspondence to: a.brand@gurdon.cam.ac.uk

This PDF file includes:

Other Supplementary Materials for this manuscript includes the following:

Materials and Methods

Fly stocks and husbandry

Drosophila melanogaster were reared in cages at 25°C, unless indicated otherwise. Embryos were collected onto yeasted apple juice plates and staged according to (*23*). For larval experiments, larvae were transferred to a fresh, yeasted food plate within 1 hour of hatching (designated 0ALH) and allowed to develop to the desired stage. To assess for *trbl* reporter expression under amino acid-deficient conditions, newly hatched larvae were instead transferred to a solution of 20% sucrose in PBS (*3*). The following stocks were used: w^{1118}, FlyTrap Line YD0837 (*trbl* reporter) (*24*), $trbl^{EP1119}$ and $trbl^{EP3519}$ (*25*), *trbl* GFSTF (*26*), UASt-GFP-Trbl (this study), *wor*-GAL4 (*27*), $insc^{MZ1407}$-GAL4 (*28*), *grh*-GAL4 (*4*), P{TRiP.HMJ02089}attP40 (UAS-*trbl*-RNAi, Bloomington *Drosophila* stock centre #42523), UASt-GFP-E2F1$_{1\text{-}230\#26}$, UASt-mRFP1-NLS-CycB$_{1\text{-}266\#17}$ (FUCCI) (*10*), UAS-mCD8-GFP (*29*), UAS-myr-Akt (*21*), UAS-dp110^{CAAX} (*22*), UAS-LT3-NDam and UAS-LT3-NDam-RpII215 (*13*), *tub*-GAL80^{ts} (*30*), UAS-dPTEN (*31*), UAS-*cdc25*-RNAi (Vienna *Drosophila* Resource Center #330033). For identification of G0-arrested NSCs, the following GAL4/split GAL4 combinations were used: *ems*-GAL4 (*32*), R49C03, R18B03^{AD}-R16H11^{DBD}, R86D02, R19B03^{AD}-R18F07^{DBD}, R19B03^{AD}-R45D04^{DBD} (Janelia FlyLight library, (*33*)).

Immunostaining

Embryos were dechorionated in 50% bleach/water for 3 minutes, fixed in 4% formaldehyde/PBS and heptane on a rolling shaker for 20 minutes and washed and stored in methanol at -20°C until use. For staining, fixed embryos were washed with 0.3% Triton X-100 (Sigma-Aldrich)/PBS (PBTx), blocked with 10% normal goat serum/PBTx and incubated with primary antibodies in PBTx overnight at 4°C. Antibodies were washed off with PBTx and replaced with secondary antibodies in PBTx for 2 hours at room temperature or overnight at 4°C. After washing, embryos were mounted in 70% glycerol/PBS. Larval brains were dissected in PBS, fixed in 4% formaldehyde/PBS for 20 minutes, and processed as described for embryos. Larval brains were mounted in Vectashield mounting medium (Vector Laboratories). The following primary antisera were used: rabbit anti-Cdc25^{String} 1:500 ((*34*)), rabbit anti-CycA 1:500 ((*35*), rb270), rabbit anti-CycB 1:500 ((*35*), rb271), guinea pig anti-Dpn 1:5,000 (kind gift of James Skeath), rat anti-Dpn 1:100 (abcam, 11D1BC7, ab195173), rabbit anti-Eg 1:500 (*36*), mouse anti-En 1:50 (DSHB, 4D9 conc.), rat anti-Ey 1:1,000 (kind gift of Patrick Callaerts), chick anti-GFP 1:2,000 (abcam, ab13970), rat anti-Mira 1:500 (kind gift of Chris Q. Doe), mouse anti-Pros 1:30 (DSHB, MR1A conc.), rabbit anti-phospho-Histone H3 Ser10 (pH3) 1:200 (Merck Millipore, 06-570), rat anti-Histone H3 phospho S28 (pH3) 1:200 (abcam, ab10543), rabbit anti-phospho-4E-BP1 1:100 (Thr37/46, Cell Signaling Technology, 236B4), rabbit anti-Run 1:1,000 (kind gift of Eric Wieschaus), rabbit anti-Tll 1:200 ((*37*), 812), rabbit anti-Msh 1:500 (*38*), rat anti-Wor 1:100 (abcam, 5A3AD2, ab196362). Primary antibodies were detected using Alexa Fluor-conjugated secondary antibodies (Life Technologies) diluted 1:500 in PBTx. For Cdc25^{String} detection, embryos were pre-incubated for 1 hour in Image-iT FX signal enhancer solution (Thermo Fisher Scientific) as described in (*34*).

Region of interest

Throughout this study, unless indicated otherwise, we assessed NSCs (identified by expression of the HES family gene *deadpan* (*dpn*)) in the thoracic segments of the ventral nerve cord (tVNC), a well-characterised region of the *Drosophila* central nervous system (**Fig. S1A**).

Assessment of cell cycle phase using FUCCI/pH3

wor-GAL4 was used to drive expression of *UASt-GFP-E2F1*$_{1-230\#26}$, *UASt-mRFP1-NLS-CycB*$_{1-266\#17}$ (FUCCI, (*10*)) in NSCs throughout development at 25^{o}C. Larval brains were dissected at 0ALH for quiescent NSCs and 48ALH for reactivated NSCs and immunostained using anti-Dpn (NSC nuclei) and anti-pH3 (mitosis marker) antisera. The combination of FUCCI probes allows discrimination between G1 (GFP positive), S (RFP positive) and G2 and M (GFP/RFP double positive) phases. pH3 labelling marks M phase specifically.

Assessment of DNA content using DAPI

10 w^{1118} brains were dissected at 0ALH, immunostained using anti-CycA and anti-Dpn antisera and stained with DAPI for 2 hours at room temperature. Brains were imaged to a depth of 35µm from the ventral surface with a confocal microscope, at 1µm intervals. Dpn^{+} NSC nuclei were detected automatically using the "Measurement" function in Volocity software (Perkin Elmer). The DAPI intensities of CycA^{+} NSC nuclei (test, G2) were scaled to the mean DAPI intensity of CycA^{-} NSC nuclei (control, G0) in the same brains.

Identification of G0 qNSCs

We identified each of the G0 qNSCs using the most recent descriptions and nomenclature published by Lacin and Truman (*12*). Each *Drosophila* NSC is named using Cartesian coordinates based on anterior-posterior and dorsal-ventral position during delamination from the neuroectoderm.

Characterisation of *wor* as a reactivation marker

Quiescent NSCs do not express *wor* at larval hatching (*8*), but expression is initiated in reactivating NSCs before they begin to divide. 100% of proliferating NSCs express *wor* by 48 hours ALH. Importantly, all dividing (pH3^{+}) NSCs are Wor^{+} (n=75 NSCs, 10 tVNCs).

Transcriptional profiling of qNSCs

In vivo transcriptional profiling was carried out using Targeted DamID (TaDa) (*13*). *wor*-GAL4 was used to drive expression of *UAS-LT3-NDam* ("Dam-only", reference) or *UAS-LT3-NDam-RpII215* ("PolII-Dam", test) in NSCs. Unlike endogenous *wor*, *wor*-GAL4 is expressed in quiescent NSCs. GAL4 activity was temporally restricted to late embryogenesis and early larval stages using *tub*-GAL80^{ts} to enrich for signal from qNSCs, although note that 10 non-quiescent NSCs/brain also express *wor*-GAL4 at these stages. Embryos were collected onto an apple juice plate for a 1 hour period and developed at 18^{o}C for 28 hours until ~Stage 16. Embryos were shifted to 29^{o}C for 10

hours to inactivate GAL80^{ts} and induce expression of TaDa constructs. ~900 L1 larval brains were dissected for each condition. The TaDa protocol and analysis were carried out as described (*13*). Two replicates were performed and amplified DNA hybridised to a Nimblegen HX1 *Drosophila* whole genome tiling microarray corresponding to genome annotation release 5 (performed at FlyChip, Cambridge, UK). Microarray data was realigned to release 6 of the Drosophila melanogaster genome for analysis, using a modified version of the FlyBase dmel_r5_to_r6_converter.pl script. Genes were deemed as expressed above a $\log_2$ ratio of 0.585 and with a false discovery rate (FDR) value below 0.01. The expressed gene list is available in **Table S2**.

In situ hybridisation against *trbl* and *cdc25^{string}* mRNA

Primers were designed in Primer3 (*39*) to amplify unique regions of *trbl* or *cdc25^{string}* from an embryonic cDNA library, with an optimum length of 24bp and T_m of 60^{o}C. Primers used were:

*trbl*_FWD 5'-TAGTCAACTATTCGTCACCAGTCT-3'
*trbl*_REV 5'-TTTTGCAATTTTCACTTACAAGAT-3'.
*cdc25^{string}*_FWD 5'-CTAAAATGCAATACTAGCCAAAAA-3'
*cdc25^{string}*_REV 5'-CAATACGATAACACCCAAACTTAG-3'

To the 5' ends of the REV primers were added the sequence 5'-CAGTAATACGACTCACTATTA-3' to allow *in vitro* transcription by T7 RNA polymerase (NEB). Approximately 1µg of amplified PCR product was used per gene for *in vitro* transcription with digoxigenin (DIG)-labelled nucleotides (NEB) for 72 hours at 18^{o}C. The transcribed products were degraded to an average length of 500bp using carbonate buffer (*40*), precipitated using ethanol and re-suspended in 10µl of DEPC water containing 0.2µl of RNAse inhibitor (Roche). DIG-labelled *in situ* probes were used at 1:500 in hybridisation buffer (*41*). Hybridisations were performed as previously described (*41*), except that the hybridisation temperature was 65^{o}C. Hybridised embryos were incubated with alkaline phosphatase (AP)-conjugated anti-digoxigenin (DIG) antibody (Roche), washed and signal detected through the chromogenic NBT/BCIP reaction. Embryos were mounted in 70% glycerol/PBS for imaging. *cdc25^{string}*-hybridised embryos were filleted and prepared as flat preparations before imaging.

RNAi-mediated knockdown of *trbl* in NSCs

Flies carrying *insc^{MZ1407}*-GAL4 (*28*) or *grh*-GAL4 were crossed to *w^{1118}* flies (control) or flies carrying P{TRiP.HMJ02089}attP40 (UAS-*trbl*-RNAi). Embryos were collected onto an apple juice plate for a 3 hour period at 25^{o}C then developed at 29^{o}C until stage 17 embryogenesis or 5ALH respectively. Embryos or dissected brains were immunostained using anti-Dpn (NSC nuclei) and anti-pH3 (mitosis marker) antisera. The total mitotic index for each embryo was quantified by expressing the total number of pH3+ cells as a percentage of the number of NSC nuclei imaged in the same brain.

Quantification of nuclear volume in *trbl* mutant larval brains

10 control (*trbl^{EP3519}* heterozygous) and 10 test (*trbl^{EP3519}* homozygous) larval brains were dissected at 0ALH and immunostained using anti-Dpn and anti-CycA (G2 *vs* G0

assessment) antisera. Dpn staining was detected and quantified in three dimensions automatically using Volocity software (Perkin Elmer) to calculate nuclear volume.

Generation of transgenic UAS-GFP-Trbl flies

The *trbl* coding sequence was PCR amplified from an embryonic cDNA library and cloned into the pUASt-NmGFP6 vector (*13*) using NotI and XbaI sites to create an N-terminal GFP fusion sequence. Transgenic flies were generated by germline injection of this construct into a w^{1118} background in the presence of the phiC31 integrase helper plasmid pBS130.

EdU incorporation and detection

Embryos: Embryos were collected onto an apple juice plate at 25°C, then dechorionated as normal in 50% bleach. After washing, embryos were air dried well in a nitex basket then incubated for 5 minutes in octane. After removal of octane, embryos were air dried briefly, then incubated for 30 minutes at room temperature in Schneider's *Drosophila* medium (Gibco, 21720-024) containing EdU at 200µg/ml. Embryos were washed with heptane, then fixed as normal on a rolling shaker. EdU detection was performed using a Click-iT EdU Alexa Fluor 647 detection kit (Molecular Probes, C10340) according to the manufacturer's instructions. Embryos were co-immunostained for Dpn (NSCs).

Larvae: For *grh*-GAL4 experiments, larvae were reared as normal until 20ALH at 29°C. At this time, larvae were washed briefly in PBS and transferred to food plates containing EdU at 50µg/ml for a further 4 hours at 29°C until dissection. Following brain fixation, EdU detection was performed using a Click-iT EdU Alexa Fluor 647 detection kit according to the manufacturer's instructions. Co-immunostaining with antibodies was performed as advised in the kit. Experiments with *wor*-GAL4 were conducted similarly, except that *tub*-GAL80^{ts} was provided in the genetic background (designated *wor^{ts}*). Embryos were reared at 18°C and larvae were shifted to 29°C at hatching to restrict GAL4 activity to quiescent stages.

Image acquisition and processing

Fluorescent images were acquired using a Leica SP8 confocal microscope and analysed using Volocity (Perkin Elmer) software. All images are single sections unless indicated otherwise. After *in situ* hybridisation, embryos were imaged by DIC on a Zeiss Axioplan microscope equipped with a Progres C10+ camera. Anterior is up in all images, unless indicated otherwise.

Images were processed for brightness and contrast using Adobe Photoshop. Figures were compiled in Adobe Illustrator.

Statistical analysis

Data were arcsin-transformed before statistical analysis if they involved percentage data. Box and whisker plots depict median (red line), interquartile range (IQR, box) and 1.5IQR below and above the first and third quartiles respectively (whiskers).

Fig. S1.

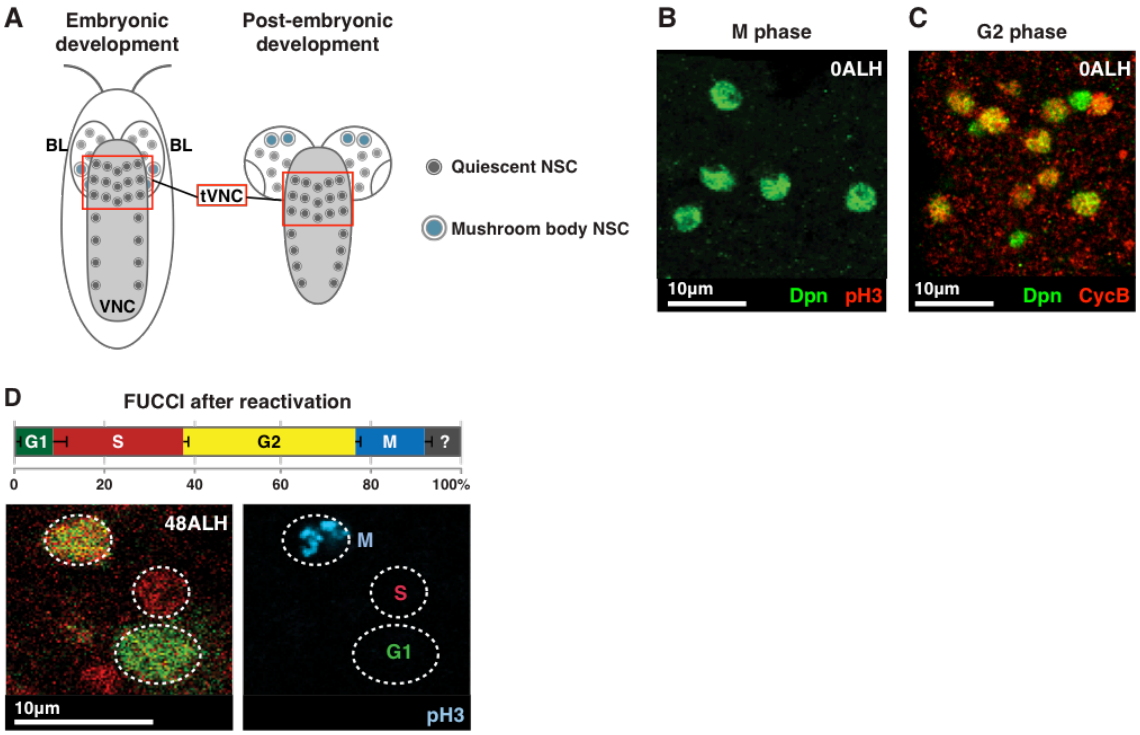

Figure S1. *Drosophila* central nervous system anatomy and NSC quiescence.
(**A**) The *Drosophila* central nervous system during embryonic (left) and post-embryonic (right) development, in ventral view. The nervous system is composed of two brain lobes (BL) and a ventral nerve cord (VNC, shaded). Red box indicates thoracic segments of the VNC (tVNC), which is the region quantified throughout this study. Mushroom body NSCs are a group of four NSCs per brain lobe that never become quiescent and act as an internal comparison.
(**B**) 0% of qNSCs (green) are $pH3^{+}$ (red). *n*=10 tVNCs, ~150 NSCs each.
(**C**) 73±0.77% of qNSCs (green) are CycB+ (red). *n*=10 tVNCs, ~150 NSCs each.
(**D**) Percentages of NSCs (outlined) in each cell cycle phase after reactivation. Colours as in (Fig. 1C). *n*=5 tVNCs, ~150 NSCs each. ?: undetermined.

Images are single section confocal images and anterior is up in this, and all subsequent figures, unless indicated otherwise.

Fig. S2.

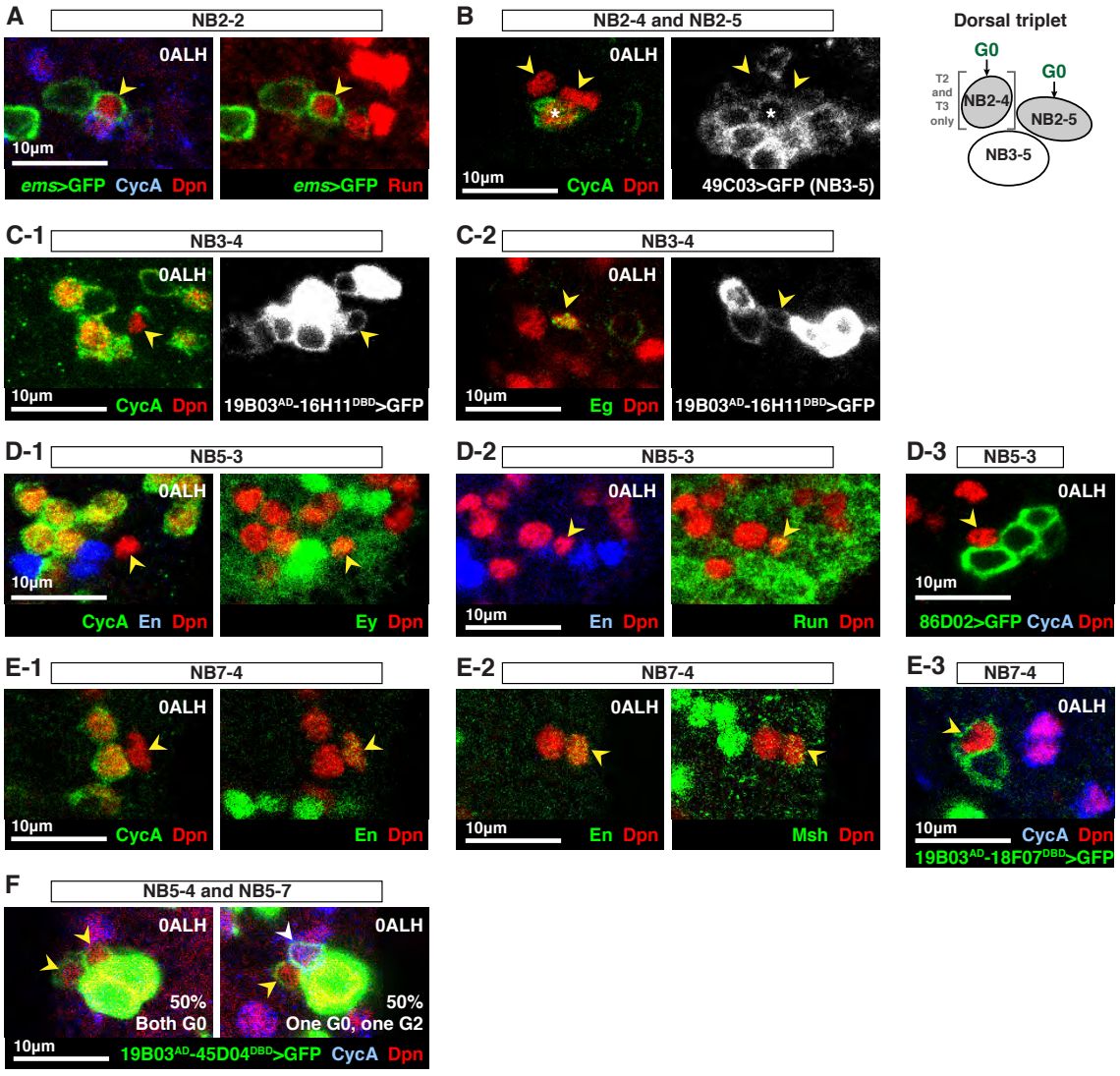

Figure S2. Identifying G0 qNSCs.
Identification of G0 qNSCs (yellow arrowheads), using diagnostic markers and GAL4 drivers according to (*12*). GAL4 drivers were crossed to a reporter line carrying UAS-mCD8-GFP to reveal expression.

(**A**) NB2-2 is located medially, is Run^{+} and labels with *ems*-GAL4. *ems*-GAL4 exhibited variable expression; see Table S1 for details.
(**B**) NB2-4 and NB2-5 are located dorsally and are part of the 'dorsal triplet', but do not label with R49C03-GAL4, which labels NB3-5 (asterisk).
(**C**) NB3-4 is a small, Eg^{+} NSC that labels with R19B03^{AD}-R16H11^{DBD}.
(**D**) NB5-3 is located in the En+ neuron file (blue). It is Ey^{+} (D-1) and Run^{+} (D-2), identifying it as NB5-3. R86D02-GAL4 labels the NB5-3 lineage, but not NB5-3 itself (D-3).

(**E**) This CycA-negative NSC is En^+ (E-1) and Msh^+ (E-2), identifying it as NB7-4. It is also labelled specifically by $R19B03^{AD}$-$R18F07^{DBD}$ (E-3). This GAL4 driver exhibited variable expression; see Table S1 for details.
(**F**) NB5-4 and NB5-7 are Run-negative NSCs labelled by $R19B03^{AD}$-$R45D04^{DBD}$ (Run staining not shown). Both NSCs are G0-arrested in 50% of hemi-segments. In the other 50% of hemi-segments, one NSC is G0-arrested and the other is G2- arrested.

NSC identities were confirmed in *n*=10 tVNCs, 3 hemi-segments each, except for NB5-4/NB5-7 for which *n*=8 tVNCs. See also Table S1.

Fig. S3.

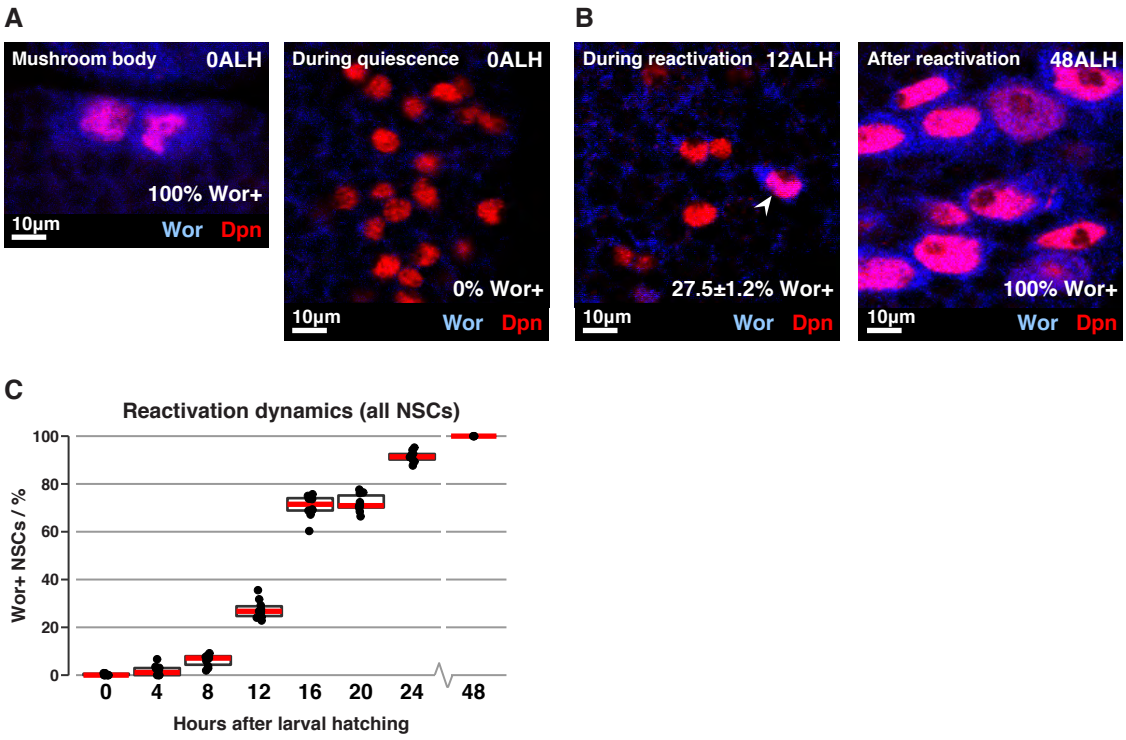

Figure S3. Wor is a reactivation marker in NSCs
(**A**) Quiescent NSCs (right) do not express Wor, in contrast to mushroom body NSCs (left) at the same developmental stage, which do not become quiescent (*n*=10 tVNCs).
(**B**) NSCs (red) begin to express Wor (blue) during reactivation. White arrowhead indicates a reactivated, Wor^+ NSC. At 12ALH, 27.5±1.2% of NSCs are Wor^+. At 48ALH 100% of NSCs are Wor^+ (*n*=10 tVNCs/time point, ~150 NSCs each).
(**C**) Quantification of Wor^+ NSCs at 4 hour intervals during post-embryonic development. *n*=10 tVNCs/time point, ~150 NSCs each.

Red lines indicate medians.

Fig. S4.

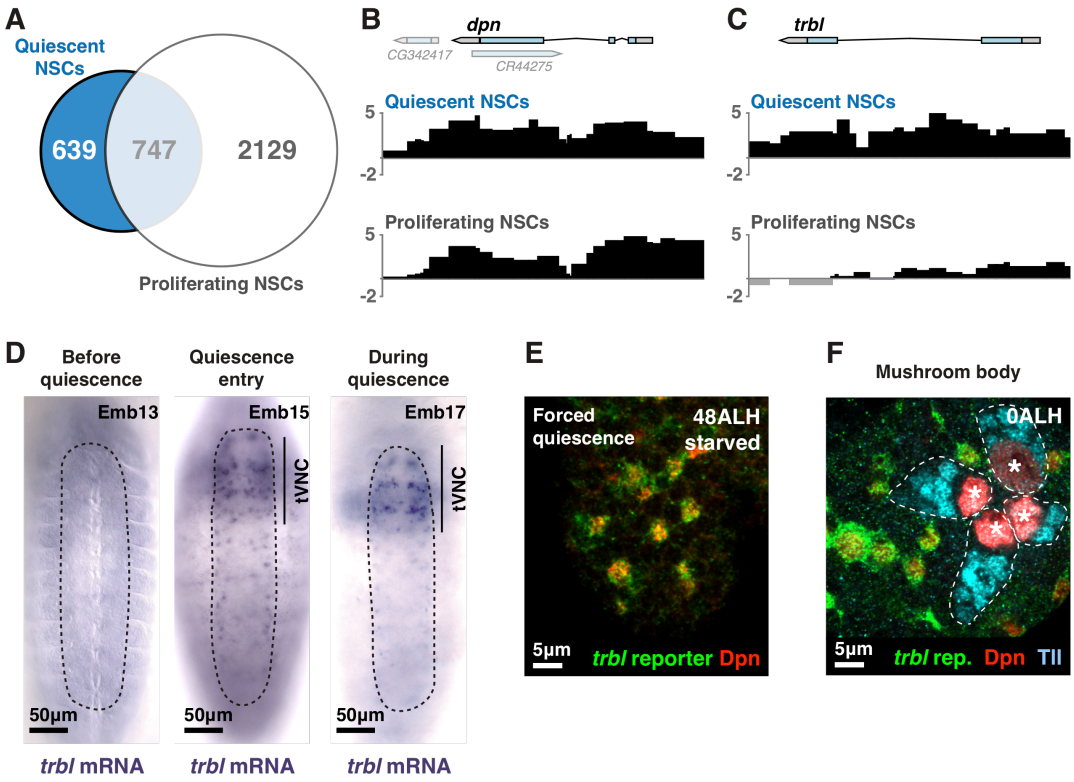

Figure S4. Quiescent NSCs express *trbl*.
(**A**) Comparison of coding genes expressed by quiescent NSCs (blue circle, this study) versus proliferating NSCs (white circle, (*13*)), assessed using TaDa.
(**B**) RNA polymerase II occupancy at *dpn* locus in quiescent *vs* proliferating NSCs. Scale bars represent $\log_2$ ratio change between test and reference samples. Proliferating NSC data from (*13*).
(**C**) RNA polymerase II occupancy at *trbl* locus in quiescent *vs* proliferating NSCs. Scale bars represent $\log_2$ ratio change between test and reference samples. Proliferating NSC data from (*13*).
(**D**) *In situ* hybridisation against *trbl* mRNA before quiescence (left), at quiescence entry (centre) and during quiescence (right). Imaged by DIC; see methods for details. Anterior is up.
(**E**) In animals starved of amino acids, NSCs remain quiescent until the animals are re-fed (*3*). 81.5±0.6% of NSCs express the *trbl* reporter at 48ALH in larvae fed an amino acid-deficient diet, compared to 0% of NSCs in larvae fed with amino acids at the same developmental stage (see right panel of Fig. 3D). n=10 tVNCs/condition, ~120 NSCs each.
(**F**) Mushroom body NSCs (white asterisks and labelled by Tll (cyan)) do not become quiescent and do not express the *trbl* reporter (green).

Fig. S5.

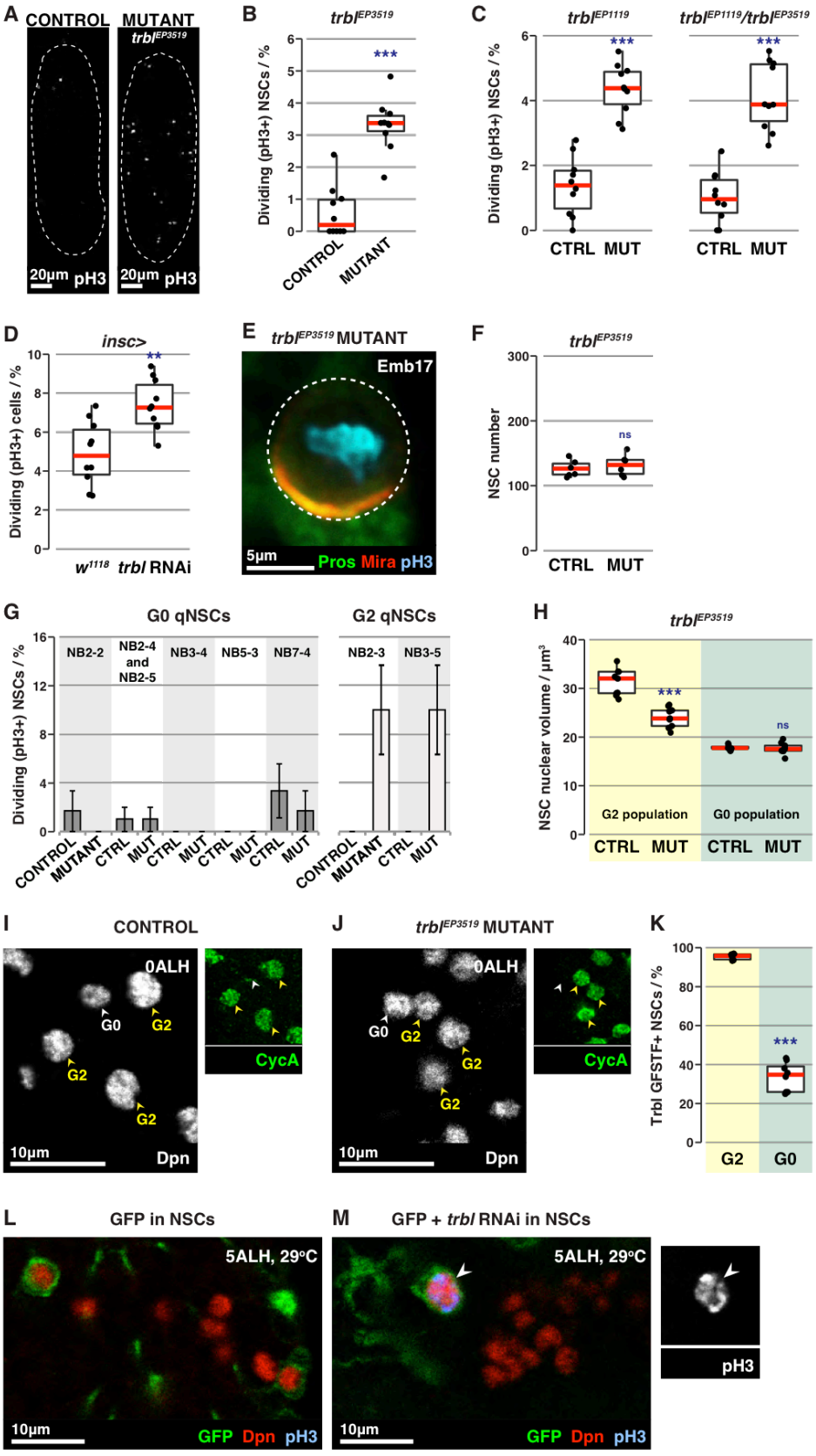
A
CONTROL
MUTANT
trblEP3519
20µm pH3
20µm pH3
B
trblEP3519
Dividing (pH3+) NSCs / %
***
CONTROL
MUTANT
C
trblEP1119
trblEP1119/trblEP3519
Dividing (pH3+) NSCs / %
***
***
CTRL MUT
CTRL MUT
D
insc>
Dividing (pH3+) cells / %
**
w1118 trbl RNAi
E
trblEP3519 MUTANT
Emb17
5µm
Pros Mira pH3
F
trblEP3519
NSC number
ns
CTRL MUT
G
G0 qNSCs
G2 qNSCs
Dividing (pH3+) NSCs / %
NB2-2
NB2-4 and NB2-5
NB3-4
NB5-3
NB7-4
NB2-3
NB3-5
CONTROL MUTANT CTRL MUT CTRL MUT CTRL MUT CTRL MUT
CONTROL MUTANT CTRL MUT
H
trblEP3519
NSC nuclear volume / µm3
***
ns
G2 population
G0 population
CTRL MUT CTRL MUT
I
CONTROL
0ALH
G0
G2
G2
G2
CycA
10µm
Dpn
J
trblEP3519 MUTANT
0ALH
G0
G2
G2
G2
CycA
10µm
Dpn
K
Trbl GFSTF+ NSCs / %
***
G2
G0
L
GFP in NSCs
5ALH, 29ºC
10µm
GFP Dpn pH3
M
GFP + trbl RNAi in NSCs
5ALH, 29ºC
10µm
GFP Dpn pH3
pH3

Figure S5. *trbl* mutant NSCs divide excessively and become smaller.
(**A**) Maximum intensity projections of control (*trbl*^{EP3519} heterozygote) and *trbl* mutant (*trbl*^{EP3519} homozygote) VNCs at embryonic stage 17, stained for the mitotic marker pH3 (grayscale).
(**B**) Quantification of dividing (pH3^{+}) NSCs in control *vs trbl*^{EP3519} mutant VNCs. *n*=10 VNCs/genotype, ~225 NSCs each. ***: $p=2.19\text{x}10^{-4}$, Mann-Whitney U test.
(**C**) Quantification of dividing (pH3^{+}) NSCs in *trbl*^{EP1119} and *trbl*^{EP1119}/*trbl*^{EP3519} mutant (MUT) VNCs at embryonic stage 17. Controls (CTRL) were heterozygous mutant embryos. *n*=10 VNCs/genotype, ~235 NSCs each. ***: $p=2.72\text{x}10^{-7}$ (left) and $p=5.11\text{x}10^{-7}$ (right), Student's *t*-tests.
(**D**) Quantification of mitotic cells in *insc*^{MZ1407}-GAL4>*w*^{1118} (control) or *trbl* RNAi (test) VNCs at embryonic stage 17 at 29^{o}C. *trbl* was knocked down in NSCs prior to normal quiescence entry. *n*=10 VNCs/genotype, ~230 NSCs each. **: $p=1.43\text{x}10^{-3}$, Student's *t*-test.
(**E**) Pros (green) and Mira (red) localisation in a dividing *trbl*^{EP3519} mutant NSC (dotted outline). pH3 (cyan) shows division plane. A crescent of Pros/Mira is clearly visible.
(**F**) Quantification of NSC number in control (*trbl*^{EP3519} heterozgote) and *trbl* mutant (*trbl*^{EP3519} homozygote) tVNCs at larval hatching. *n*=6 tVNCs/genotype. *ns*: $p>0.05$, Student's *t*-test.
(**G**) Percentage of dividing G0 or G2 qNSCs in control (CTRL, *n*=10) *vs trbl*^{EP3519} mutant (MUT, *n*=10) tVNCs with 6 lineages each, at embryonic stage 17. NB2-4 and NB2-5 were not distinguished. Data presented as mean±S.E.M.
(**H**) Quantification of nuclear volume of G2 and G0 qNSCs in control *vs trbl*^{EP3519} mutant tVNCs. *n*=9 tVNCs/genotype, ~75 NSCs each. ***: $p=9.68\text{x}10^{-6}$, Student's *t*-test. *ns*: $p>0.05$.
(**I** and **J**) Comparison of NSC size in control (I) *vs trbl*^{EP3519} mutant (J) tVNCs. Nuclei were visualised by immunostaining for Dpn (grayscale); G2 or G0 qNSCs were determined by staining for CycA (green). G2, but not G0, NSCs become smaller in *trbl* mutants.
(**K**) Percentages of G2 and G0 quiescent NSCs expressing Trbl protein (Trbl-GFSTF is an epitope-tagged Trbl protein driven from its own locus (*26*)). *n*=7 tVNCs, ~120 NSCs each. ***: $p=4.86\text{x}10^{-7}$, unequal variances *t*-test.
(**L** and **M**) Conditional knockdown of *trbl* in NSCs that have already entered quiescence using *grh*-GAL4. Control NSCs (L) never divide. In *trbl* knockdown VNCs (M), NSCs leave quiescence and begin to divide (pH3, blue/grayscale, arrowhead, *n*=5/15 brains).

Fig. S6.

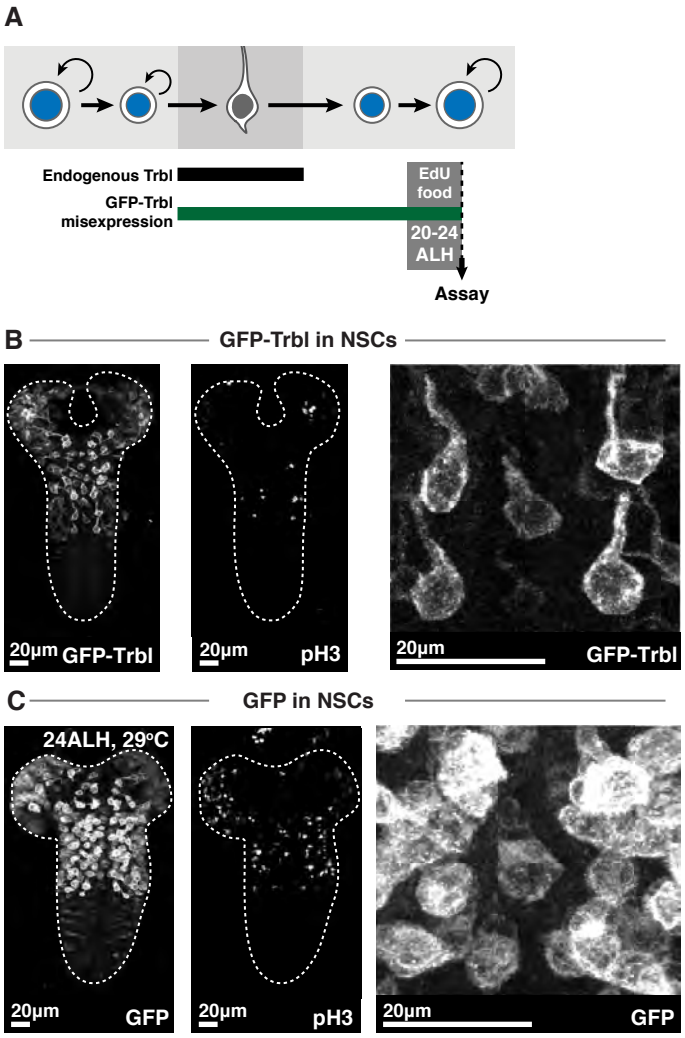

Figure S6. Trbl is sufficient to maintain G2 quiescence.
(**A**) GFP-Trbl misexpression strategy using *grh*-GAL4. Larvae were transferred to EdU-containing food 4 hours prior to dissection.
(**B** and **C**) *grh*-GAL4 was used to express GFP-Trbl (test, B) or mCD8-GFP (control, C) in NSCs. GFP-Trbl-expressing NSCs retain a primary process and divide less (pH3), while control NSCs are spherical and divide more. Note that $pH3^{+}$ cells in (B) are NSCs that do not express GFP-Trbl. Maximum intensity projections.

Fig. S7.

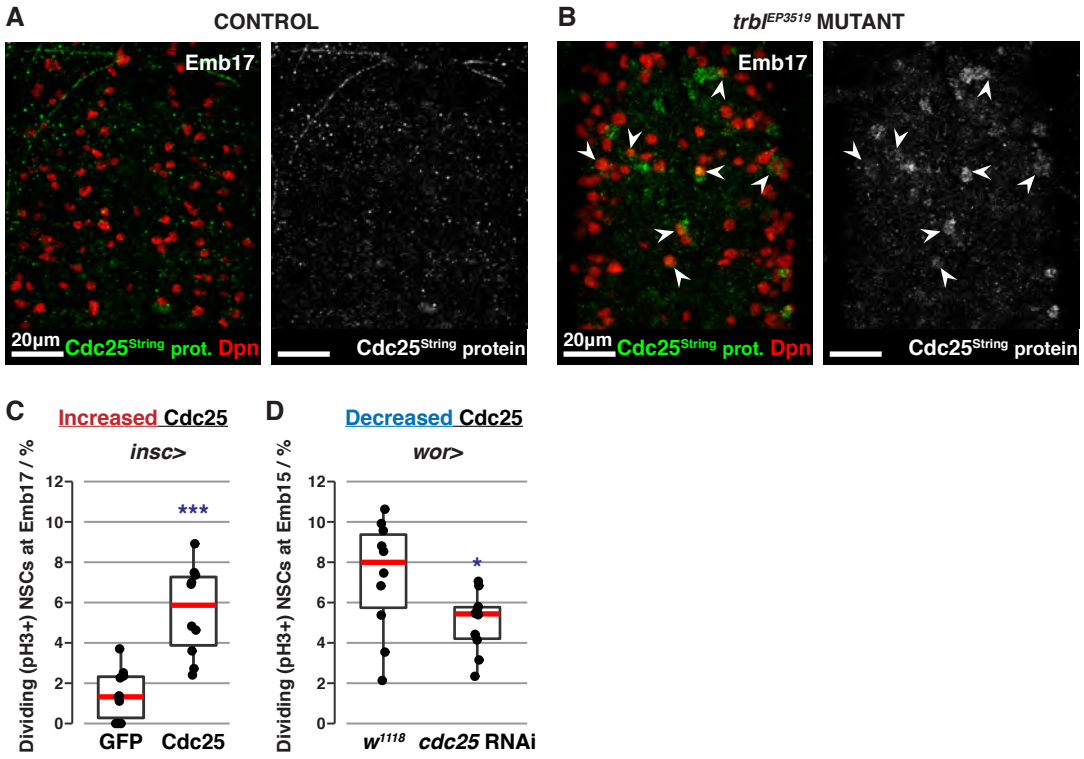

Figure S7. Trbl induces quiescence entry by decreasing Cdc25^{String} protein.
(**A-B**) Cdc25^{String} protein abundance (green/grayscale) in control (*trbl*^{EP3519} heterozygote) *vs trbl*^{EP3519} mutant NSCs at embryonic stage 17. Control NSCs do not express Cdc25^{String} protein after quiescence entry (B). In contrast, *trbl*^{EP3519} mutant NSCs express Cdc25^{String} protein (arrowheads, C). Maximum intensity projections.
(**C**) Quantification of dividing (pH3+) NSCs in control tVNCs *vs* test tVNCs misexpressing Cdc25^{String} at embryonic stage 17. *insc*^{MZ1407}-GAL4 was used to misexpress Cdc25^{String} in NSCs. n=10 tVNCs/genotype, ~120 NSCs each. ***: p=1.57x10^{-4}, unequal variances t-test.
(**D**) Quantification of dividing (pH3+) NSCs in control tVNCs *vs cdc25*^{string} knockdown tVNCs at embryonic stage 15. *wor*-GAL4 was used to express *cdc25*^{string} RNAi in NSCs. n=10 tVNCs/genotype, ~120 NSCs each. *: p=0.04, Student's t-test.

Fig. S8.

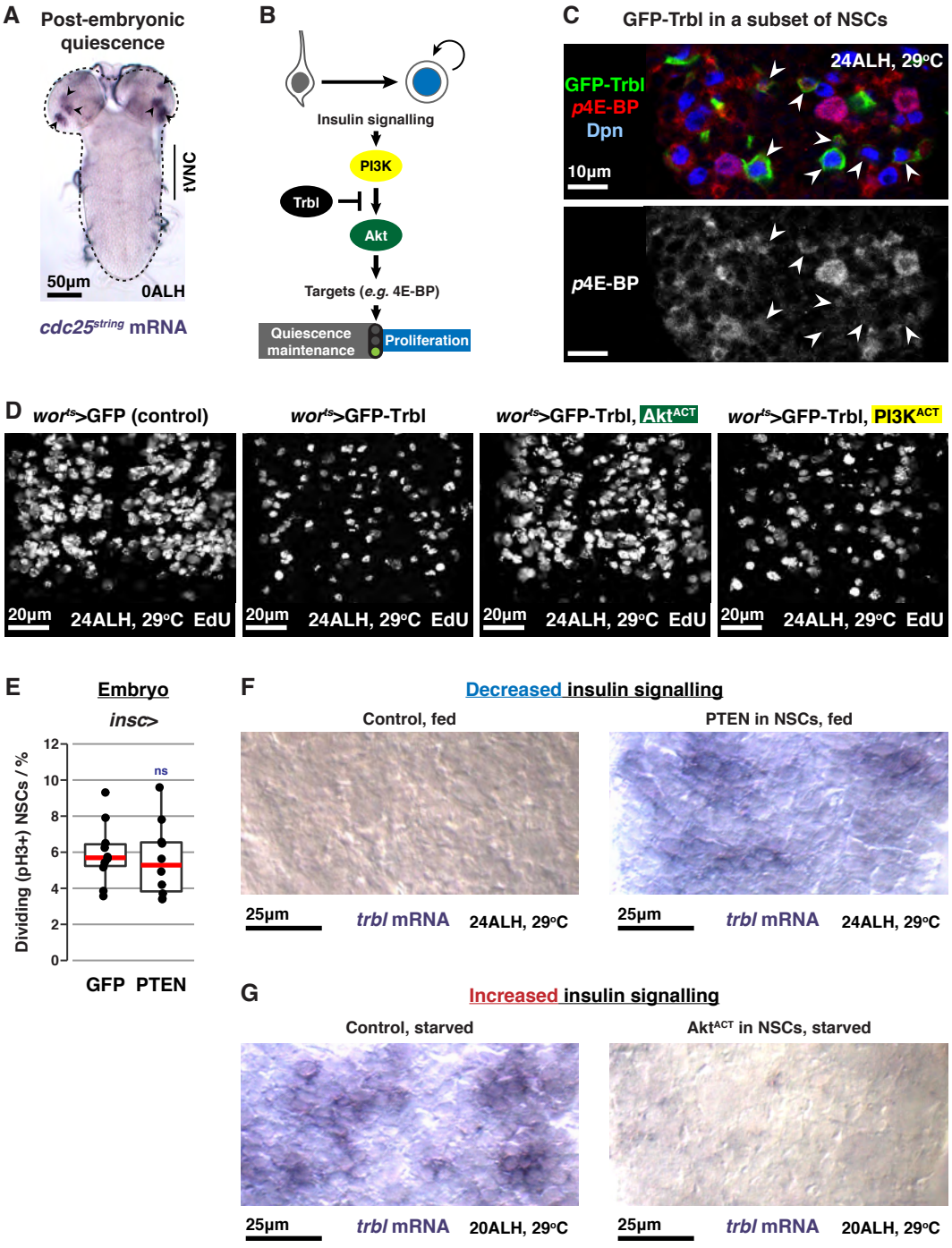

Figure S8. Reciprocal antagonism between Trbl and the insulin signalling pathway.

(**A**) *In situ* hybridisation against *cdc25*^{string} mRNA in the post-embryonic brain at 0ALH. Quiescent NSCs in the tVNC no longer transcribe *cdc25*^{string} after hatching. Proliferative

mushroom body NSCs in the brain lobes (arrowheads) still transcribe *cdc25*^{string} and act as an positive control for the probe. Imaged by DIC.
(**B**) Trbl can bind and prevent Akt activation in the insulin signalling pathway (*20*).
(**C**) GFP-Trbl (green) was expressed in a subset of NSCs (blue) using the *grh*-GAL4 driver. Insulin/TOR pathway effector *p*4E-BP in red/grayscale. GFP-Trbl-expressing NSCs (arrowheads) have reduced *p*4E-BP staining compared to neighbouring control NSCs.
(**D**) Epistasis experiments between GFP-Trbl and Akt^{ACT} or PI3K^{ACT}. Maximum intensity projections of EdU incorporation (grayscale) in tVNCs. *wor*-GAL4 and *tub*-GAL80^{ts} were used to express the indicated transgenes from larval hatching. Akt^{ACT}, but not PI3K^{ACT}, rescues reactivation in GFP-Trbl-expressing NSCs.
(**E**) Quantification of dividing (pH3+) NSCs in control *vs* test tVNCs misexpressing PTEN at embryonic stage 15. *insc*^{MZ1407}-GAL4 was used to misexpress PTEN in NSCs. Reduced insulin signalling has no effect on embryonic NSC proliferation. n=10 tVNCs/genotype, ~120 NSCs each. *ns*: $p>0.05$, two-tailed t-test.
(**F**) *In situ* hybridisation against *trbl* mRNA in control brains (*grh*-GAL4 crossed to *w*^{1118}) *vs* test brains (*grh*-GAL4 driving PTEN expression in NSCs). PTEN expression reduces insulin pathway activity and increases *trbl* transcription in the tVNC. Imaged by DIC.
(**G**) *In situ* hybridisation against *trbl* mRNA in control brains (*grh*-GAL4 crossed to *w*^{1118}) or test brains (*grh*-GAL4 driving Akt^{ACT} expression in NSCs) under amino acid-deficient conditions. Control NSCs (left) express *trbl*. Akt^{ACT} expression (right) increases insulin pathway activity and downregulates *trbl* transcription in the tVNC. Imaged by DIC.

Table S1.

G0 cell	Diagnostic GAL4 drivers	Molecular marker(s)	Other features
NB2-2	Labelled by *ems*-GAL4. This GAL4 driver labelled this NSC variably (~40% of hemi-segments, *n*=10 brains, 3 hemi-segments each).	Run^+.	Medial position, close to midline.
NB2-4	Part of the 'dorsal triplet' of NSCs but not labelled by R49C03-GAL4.	*n/a*.	Dorsal position in tVNC; part of the 'dorsal triplet'. Absent in T1 hemi-segment.
NB2-5	Part of the 'dorsal triplet' of NSCs but not labelled by R49C03-GAL4.	*n/a*.	Dorsal position in tVNC; part of the 'dorsal triplet'.
NB3-4	Labelled by $R19B03^{AD}$-$R16H11^{DBD}$.	Eg^+.	Very small.
NB5-3	Progeny are labelled by R86D02-GAL4.	Ey^+ Run^+.	Very small.
NB5-4	Labelled by $19B03^{AD}$-$45D04^{DBD}$ and does not express Run. *n*=8 tVNCs.		*n/a.*
NB5-7	Labelled by $19B03^{AD}$-$45D04^{DBD}$ and does not express Run. *n*=8 tVNCs.		*n/a.*
NB7-4	Labelled by $R19B03^{AD}$-$18F07^{DBD}$. Every NSC labelled by this driver is G0-arrested. However, this driver does not label NB7-4 in every segment.	En^+ Msh^+.	*n/a.*

Table S1. Features used to identify G0 qNSCs.
All observations were confirmed in *n*=10 tVNCs, 3 hemi-segments each, unless indicated otherwise. NSCs were assessed at 0ALH. G0 qNSCs were defined as being Dpn^+ CycA-negative.

Additional Data

Supplementary Table S2 (separate file)
Genes expressed in quiescent NSCs.

Supplemetary Table S3 (separate file)
GO terms associated with quiescent NSC genes.

Supplementary References

23. J. A. Campos-Ortega, V. Hartenstein, *The Embryonic Origin of Drosophila melanogaster* (1985).

24. A. T. Quiñones-Coello *et al.*, *Genetics*. **175**, 1089–1104 (2007).

25. P. Rørth *et al.*, *Development*. **125**, 1049–1057 (1998).

26. S. Nagarkar-Jaiswal *et al.*, *eLife*. **4**, e05338 (2015).

27. R. Albertson, C. Chabu, A. Sheehan, C. Q. Doe, *J. Cell. Sci.* **117**, 6061–6070 (2004).

28. L. Luo, Y. J. Liao, L. Y. Jan, Y. N. Jan, *Genes & Development*. **8**, 1787–1802 (1994).

29. T. Lee, L. Luo, *Neuron*. **22**, 451–461 (1999).

30. S. E. McGuire, P. T. Le, A. J. Osborn, K. Matsumoto, R. L. Davis, *Science*. **302**, 1765–1768 (2003).

31. H. Huang *et al.*, *Development*. **126**, 5365–5372 (1999).

32. A. Estacio-Gómez *et al.*, *Development*. **140**, 2139–2148 (2013).

33. H.-H. Li *et al.*, *Cell Rep*. **8**, 897–908 (2014).

34. S. Di Talia *et al.*, *Curr. Biol.* **23**, 127–132 (2013).

35. W. G. Whitfield, C. Gonzalez, G. Maldonado-Codina, D. M. Glover, *EMBO J.* **9**, 2563–2572 (1990).

36. R. Dittrich, T. Bossing, A. P. Gould, G. M. Technau, J. Urban, *Development*. **124**, 2515–2525 (1997).

37. D. Kosman, S. Small, J. Reinitz, *Dev. Genes Evol.* **208**, 290–294 (1998).

38. T. Isshiki, M. Takeichi, A. Nose, *Development*. **124**, 3099–3109 (1997).

39. S. Rozen, H. Skaletsky, *Methods Mol. Biol.* **132**, 365–386 (2000).

40. K. H. Cox, D. V. DeLeon, L. M. Angerer, R. C. Angerer, *Developmental Biology*. **101**, 485–502 (1984).

41. G. S. Wilkie, A. W. Shermoen, P. H. O'Farrell, I. Davis, *Curr. Biol.* **9**, 1263–1266 (1999).